IEEE Access
Multidisciplinary ⋮ Rapid Review ⋮ Open Access Journal

Received January 20, 2021, accepted January 24, 2021, date of publication January 28, 2021, date of current version February 8, 2021.

Digital Object Identifier 10.1109/ACCESS.2021.3055247

Syncretic Application of IBAS-BP Algorithm for Monitoring Equipment Online in Power System

ZHENGGUANG LIU[1], (Student Member, IEEE), QINYUE TAN[1], (Senior Member, IEEE), YUBO ZHOU[1], AND HENGSHAN XU[2]

[1]Department of Power and Electrical Engineering, Northwest A&F University, Xianyang 712100, China
[2]College of Electrical Engineering and New Energy, China Three Gorges University, Yichang 443002, China

Corresponding author: Qinyue Tan (qinyuetan@nwsuaf.edu.cn)

This work was supported in part by the National Natural Science Foundation of China under Grant 51577157, and in part by the Natural Science Basic Research Program of Shaanxi Province under Grant 2019JM-357.

ABSTRACT With the integration and development of sensor technology and control technology, the construction of smart grid is in the ascendant. But existing technology is still insufficient in the field of equipment monitoring. Therefore, it is difficult to accurately determine if SF_6 breaker or other equipment have faults in its operational mechanisms which can cause false action and thus impact the safety of power grids. In this paper, the IBAS (Improved Beetle Antennae Search) algorithm and the BP neural network are combined and used in the monitoring system for the first time. To improve the beetle search algorithm, a single beetle is improved into a population in the iterative process of algorithm. The measured opening (closing) current data is used to verify the accuracy of different algorithms. The results show that compared with PSO-BP (particle swarm optimization, PSO) model, GA-BP (genetic algorithm, GA) model and BAS-BP model, the IBAS-BP model not only effectively avoids the possibility of local minimums but also has higher prediction accuracy and better robustness. The number of iterations in the IBAS-BP algorithm is only 38, and the average error is only 0.1%. According to this, it is possible to make real-time diagnosis of faulty states in SF_6 breaker including iron core jams, low operating voltages, poor contact of auxiliary switches, jammed operating mechanisms, and barometer failures in SF_6. At the same time, the IBAS-BP algorithm can be applied to wind turbine power prediction and other occasions since model regression determination coefficient R^2 of the training set is up to 0.9753 and the relative average error is only 0.25%. The results prove that the IBAS-BP algorithm has obvious advantages and fairly good universality. It can be further promoted and applied to power systems to provide reference for optimizing the online monitoring of power equipment.

INDEX TERMS Smart grid, intelligent monitoring, SF_6 breaker, risk prediction, fault diagnosis, wind power, IBAS-BP algorithm.

I. INTRODUCTION

The introduction of a large number of renewable energy sources makes the construction of Smart grid face two major challenges [1], [2]. On the one hand, it is more difficult for signal acquisition, transmission [3], and processing [4]; on the other hand, the connection and protection between devices [5] has also become more difficult in power systems [6]. In order to effectively solve the above problems, it is necessary to implement online monitoring of the status of power devices [7], [8]. There are two major problems in the monitoring system [9]. On the one hand, smart sensors are only applied to the interface between technologies and the market [10]. The lack of universal algorithms makes the performance of power equipment monitoring in fault diagnoses unsatisfactory [11], [12]. For distributed power equipment such as wind turbines and circuit breakers, we need to diagnose the internal changes of the entire equipment [13] and predict possible damages [14]. Based on the above dilemma, Gao *et al.* [15] have proposed that the improved LMD and HMM be used for multi-scale fault diagnoses of equipment, and, the finite difference iterative forecasting model proposed by Liu *et al.* [16] has also been verified in power load forecasting and life prediction of wind turbine gearboxes [17].

The associate editor coordinating the review of this manuscript and approving it for publication was Wentao Fan.

In addition to these algorithms, the development of other search algorithms has also become more and more popular in recent years [18].

Algorithms can expand the functions of smart meters in the energy market. The application of the PSO (BP-particle swarm optimization, PSO) algorithm for partial discharge diagnoses of transformers, motor optimization designs and transfer [19], [20] has verified the high efficiency and precision of decision-making. Song *et al.* [21] used quantum-behaved particle swarm optimization to accurately predict the load of the power system, and, the delay problem of the sensor can also be effectively solved [22]. But the (particle swarm optimization, PSO) PSO algorithm has the problem of slow iteration speed and long processing [23]. The GA (genetic algorithm, GA) algorithm also has excellent performance in wind power prediction [24] and permanent magnet motor speed control [25]. Li *et al.* [26] have used the genetic algorithm for fault diagnosis in rolling bearing, and, Ousama Osman *et al.* have also used the GA in Soft Fault Identification in Wired Networks application [27]. But the GA is complicated and difficult to promote [28]. The BAS (beetle antennae search, BAS) algorithm performs well in the classification and diagnoses of numerical prediction in recent years [29]. Wu *et al.* [30] and Cheng *et al.* [31] had applied the BAS algorithm for the path planning of mobile robots,but, due to the initial value of beetle [32], the algorithm is easy to fall into the local optimum [33]. Jiang *et al.* [34] proposed to improve this disadvantage through different search strategies, but it cannot completely solve the problem.

This research tries to improve the traditional search method of BAS by firstly proposing the IBAS (improved beetle antennae search, IBAS) algorithm. The individuals in the original BAS algorithm is changed into a population to reduce errors caused by the randomness of the initial positions in the original BAS algorithm. By combining it with the BP neural network, the generalized IBAS-BP intelligent algorithm is thus obtained. It is used in SF6 circuit breaker fault diagnoses and wind turbine power predictions. Applying this IBAS-BP algorithm can promote the integration of energy flow and information flow in smart grids.

II. IBAS-BP ALGORITHM

A. IBAS SEARCH ALGORITHM

In the monitoring of traditional power equipment, BP network can be optimized by search algorithms. BAS can effectively classify and diagnose the fault status of power equipment via the improved BP network algorithm [20], [21]. The BAS algorithm can realize prediction and classification when the function gradient information is unknown. However, due to the randomness of the initial positions and directions of the beetle, it is easy to cause the BAS algorithm to fall into a local optimum, leading to misjudgments of results.

In order to further improve the accuracy of BAS algorithm optimization, the individual beetles in the original algorithm should be optimized into a population, and then optimize BP neural networks to improve the prediction accuracy of BP neural networks. Using the massive data collected by sensors as the input variables of BP networks, the IBAS algorithm can shorten the iteration process and time. The states of most power equipment including circuit breakers, transformers, and switches can be accurately determined and evaluated.

The specific steps are as follows:

1)Construct a k-dimensional random vector to express the orientation of each beetle's whiskers and normalize it:

$$\begin{cases} \mathrm{b} = \dfrac{rand(k,1)}{||rand(k,1)||} \\ k = M^*N + N^*L + N + 1 \end{cases} \tag{1}$$

In this formula, *rand ()* is a random function. In the BP shallow network model, the number of input layer neurons is M, which is the data collected by the sensor. The number of output layers is L, which is the result we need. The number of hidden layer neurons is N, and the model search dimension is: $k = M * N + N * L + N + 1$. The numbers of network input layers and output layers can be determined according to the required feature quantity. By verifying the *fitness* of the BP neural network of different hidden layers, the numbers of hidden layer neurons can be selected. The numbers of iterations can be based on specific status judgments that generally do not exceed 100.

2)Space coordinates of left and right of a single longicorn:

$$\begin{cases} x_{ir} = x^t + d^{it} \cdot condition \\ x_{il} = x^t - d^{it} \cdot condition \end{cases} \tag{2}$$

The original BAS algorithm is improved as the IBAS algorithm has changed one single beetle into a beetle population. x_{ir} indicates that the right whisker space position of the *i-th* beetle after the *t-th* iteration, and x_{il} indicates the left whisker space position of the*i-th* beetle after the *t-th* iteration. d^{it} is the distance between the left whisker and right whisker of this beetle, x^t represents the centroid coordinates of the location of beetle *i-th*. The comparison of the intensity of the two beetles can determine the direction of the beetle, shorten the iterative speed of the algorithm, and reduce monitoring time. The *condition* in this article is set as b.

3) Determine the intensity of left and right whiskers

Use the fitness function to determine the odor intensity of the left and right whiskers, and, the locations of the left and right longhorn whiskers can be updated by the equations below.

$$\begin{cases} x^{it+1} = x^{it} - \delta^{it} * b * sing[f(x_{ir}) - f(x_{il})] \\ fitness = \dfrac{1}{N}\displaystyle\sum_{j=1}^{N}(t_{sim(j)} - y_j)^2 \end{cases} \tag{3}$$

In this formula, δ^{it} represents the step factor corresponding to the *i-th* longhorn at the *t-th* iteration and *sing ()* is the sign determination function. In the fitness function, y_j represents the output value of the *j-th* sample, and $t_{sim(j)}$ represents the actual value of the *j-th* sample. By verifying the *fitness* of different hidden layer BP neural networks, the accuracy and

precision of power equipment condition monitoring can be guaranteed. Let the number of beetles in the population be S and the position vector of each beetle be composed of the weight and threshold of the BP network. The dimension of the individual position vector is D. It can be obtained that the longicorn population can be represented by an S×D matrix.

$$P(S,D)=\begin{vmatrix} \omega_1^1, & \omega_2^1\cdots\omega_i^1, & b_1^1, & b_2^1\cdots b_i^1 \\ \omega_1^2, & \omega_2^2\cdots\omega_i^2, & b_1^2, & b_2^2\cdots b_i^2 \\ \omega_1^j, & \omega_2^j\cdots\omega_i^j, & b_1^j, & b_2^j\cdots b_i^j \end{vmatrix} \tag{4}$$

4) Determine the step size factor

Step size factor is used to control the search range of a single beetle. In order to prevent search area from being too small and local minimum values appearing, a larger initial step size can be set. To ensure the refinement of the search, this paper uses linearly decreasing weights to set step sizes.

$$\begin{cases} \delta^{it+1}=\delta^{it}*\eta_n & t=(0,1,2,\cdots,n) \\ \eta_n=\eta_1+0.01(n-1), & \eta\in[0,1] \end{cases} \tag{5}$$

η in the formula is the step size attenuation coefficient and the number should be taken from [0,1]. Up to now, the step factor value setting has not been guided by a complete theoretical system. After subsequent parameter adjustment and simulation verification, we find that when factor η is 0.95 and the initial step size is $\eta = 4$, the iteration speed is the fastest. In the BAS algorithm, the step size can be adjusted to ensure that the BAS algorithm has the highest asymptotic convergence probability. According to this, the optimization effect of the BAS algorithm is related to the parameters settings of δ and η in equation (5).

It can be seen from Figure 1(a)(b) that under the same initial step size δ, the number of iterations will decrease as the attenuation factor increases. When η takes a value less than 0.95, it will cause the algorithm to fall into the local maximum Excellent, more than 0.95 will increase the number of iterations. Therefore, from a comprehensive point of view, the convergence effect is best when 0.95 is taken. It can be seen from Figure 1(b) that the larger the initial step size δ, the greater the number of iterations. When δ is less than 4, the algorithm will fall into a local minimum. Therefore, when attenuation factor η takes the values of 0.95, the initial when the step size is 4, the IBAS-BP algorithm has the best convergence. The IBAS-BP neural network with optimized parameters can be used for training and fault diagnoses.

B. OPTIMAL SOLUTION GENERATION

Initialize the location of each beetle in the beetle herd. The initial position of each beetle should be a random number between −0.5 and 0.5. and be saved in the *best A* set. At the same time, the global best adaptation values of all the longhorns at this time are recorded in the *best fitness A* set according to fitness functions. After that, the location of each beetle is iteratively updated according to equation (3). After each update is completed, the left and right positions must be

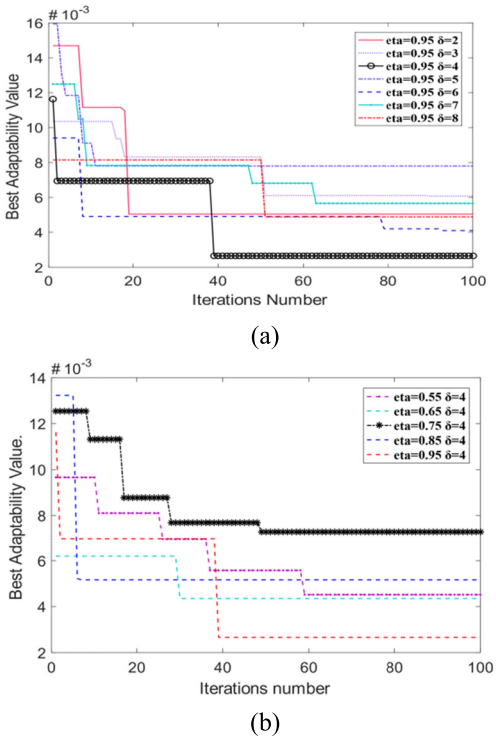

FIGURE 1. Fitness curves for different attenuation factors.

iterated according to equation (4) to obtain the corresponding fitness function values. Then, the *bestA* set and *best fitness A* set are updated in time. Finally, by comparing the global best fit values of the entire beetle population in the two sets, the best initial position of the whole beetle population *best B* and the best fitness value of the population *best fitness B* are obtained, which is the optimal solution.

Repeat the above process continuously until the fitness function value reaches the set range (this article takes 0.001) or iterates to the maximum number of times (It is set to 100 in this article), the solution set in *best B* at this time can be regarded as the best solution obtained by training. That is the optimal initial weight and threshold of the BP neural network. After that, secondary training and learning is carried out. The specific flowchart is shown in Figure 2.

III. IBAS-BP ALGORITHM OPTIMIZES EQUIPMENT MONITORING

By applying the IBAS-BP algorithm to power grid equipment, data from existing sensors and smart meters can be used to extract features required by the algorithm to achieve fault diagnoses. Information exchange and transmission between equipment ports and monitoring ports can be realized. The digital drama in the smart meters is used to make decisions in collaboration with the IBAS-BP algorithm and fault diagnoses can be realized. The diagram of the online equipment monitoring system is shown in Figure 3. Verification shows that the IBAS-BP algorithm has shorter iteration time and faster iteration speeds, which can effectively reflect the internal trend changes of components in the entire power grid.

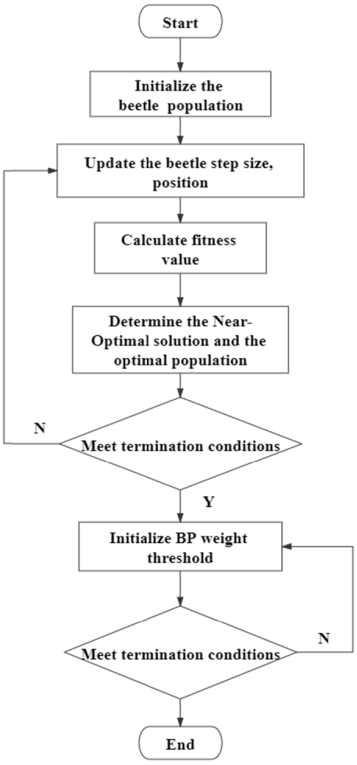

FIGURE 2. BP neural network prediction flowchart based on IBAS algorithm.

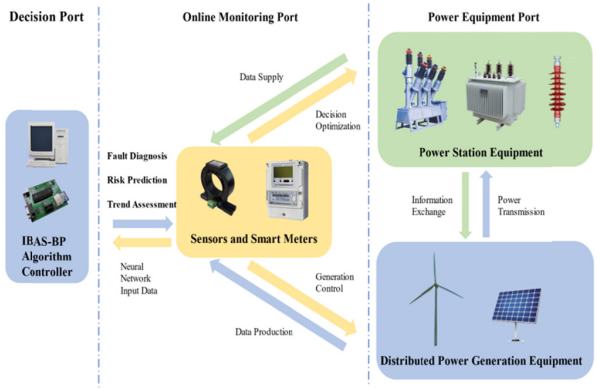

FIGURE 3. Intelligent grid monitoring system optimized by IBAS-BP algorithm.

This paper selects two applications of SF6 circuit breakers and wind turbine motor temperature predictions to demonstrate the monitoring and optimizing of equipment by the IBAS algorithm.

A. SF6 CIRCUIT BREAKER FAULT DIAGNOSIS

SF6 circuit breakers play an important role in the safe and stable operation of the power grid. Routine inspections cannot realize the real-time monitoring of SF6 circuit breaker statuses as well as the IBAS-BP algorithm and the data collected by the current sensor when SF6 circuit breakers are switched on. The eight characteristic parameters $t_1 \sim t_5$, $I_1 \sim I_3$ are used as the 8 input parameters of the BP neural network input

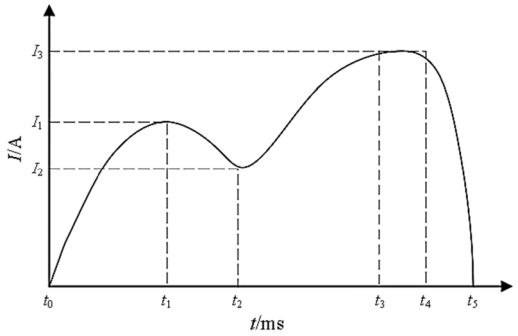

FIGURE 4. Normal current wave form of the opening (closing) coil.

layer. The extracted current characteristics of SF6 circuit breaker are shown in Figure 4.

The 3AP1FG (110kV) SF6 high voltage circuit breaker is used for testing, and the normal and simulated fault state operations are collected under no-load conditions. 200 groups of opening (closing) current sensor data are recorded with 30 groups for each fault type. Eliminated are 17 groups of bad data sets caused by weather conditions and human operations, 3 out of 17 poor data sets and 3 redundant data sets. Then, 25 groups from each fault type are selected as training samples, and the other 5 groups of data are used to test the characteristics of the network. Table 1 records part of the data.

In the above data: ZC in the fault type column is normal; HKS means that the iron core is stuck; GD means that the operating voltage is too low; FK means that the auxiliary switch has poor contact; CKS means that the operating mechanism is stuck; BF means SF6 the barometer is malfunctioning; 0 means that this fault has not occurred, and, 1 means that this fault has occurred. The output values of the algorithm are expressed by codes and are in the range of 0∼1. The larger the values, the greater the probability of failures. High-voltage circuit breaker fault types and their codes are shown in Table 1.

IBAS-BP fault diagnosis results are recorded in Table 2 and the six common SF6 circuit breaker faults are recorded in binary system by BCD codes. The intelligent algorithm represented by the IBAS-BP algorithm can effectively diagnose the fault types of SF6 circuit breakers, which proves the possibility of applying the algorithm in realizing fault classification and online monitoring.

B. WIND TURBINE POWER PREDICTION

The working places of wind turbines often have abnormal weather conditions such as turbulence and storms, which breaks the safe working limits of wind turbines and can cause damage. Therefore, wind turbines will use sensors to detect the health of wind turbine components. However, it is difficult for sensors to cover all parts of the fans, and, too many sensors will increase maintenance burdens. Besides, sensors can only monitor the results of failures, and cannot actively adjust and prevent damage when encountering special weather conditions.

TABLE 1. Types and codes of mechanical faults in SF_6 breaker.

Number	I1 (A)	I2 (A)	I3 (A)	T1 (ms)	T2 (ms)	T3 (ms)	T4 (ms)	T5 (ms)	Fault Type	Output
1	0.71	0.62	0.83	25.52	31.59	39.71	41.85	42.95	ZC	000001
2	0.59	0.51	0.62	25.78	30.93	39.72	41.34	42.47	GD	000010
3	0.71	0.62	0.85	23.93	38.43	44.05	48.70	52.66	FK	000100
4	0.71	0.62	0.85	28.77	35.77	43.66	45.95	46.92	HKS	001000
5	0.73	0.61	0.91	25.83	31.36	39.82	44.41	46.05	CKS	010000
6	0.72	0.64	0.87	25.96	33.45	41.08	45.52	56.93	BF	100000

TABLE 2. Simulation results of the IBAS-BP algorithm.

Number	Experimental Result						Fault Type	BCD
1	0.9988	0.0028	-0.0038	0	0.0008	-0.0027	ZC	001
2	0.0013	0.9991	0.0060	-0.0057	-0.0008	0.0034	GD	010
3	-0.0045	0.0046	1.0016	-0.0054	0.0035	0.0070	FK	011
4	0.0002	-0.0002	-0.0014	0.9990	0.0023	0.0015	HKS	100
5	-0.0012	-0.004	0.0047	0.0031	0.9935	0.0041	CKS	101
6	0.0014	0.0201	0.0096	0.0045	0.0018	0.9952	BF	110

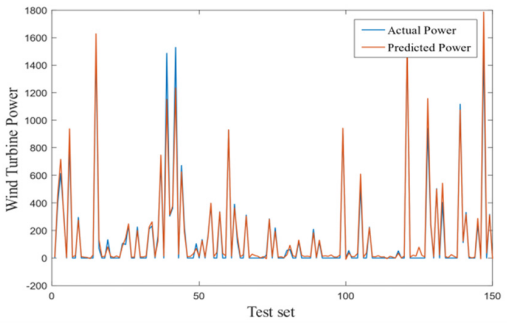

FIGURE 5. Fitting results of training based on the IBAS-BP neural network.

Based on the above problems, a variety of sensor data collected for experiments are chosen in this paper as 1,200 sets of data are recorded from experimental training sets and 150 sets of data are recorded on test sets to test the actual prediction effects of the algorithm. All that is needed is to select wind speeds, generator speeds, wind directions, blade angles, ambient temperatures, engine room temperatures, gear box oil temperatures, hydraulic oil temperatures, U1 winding temperatures, gear box shaft 1 temperatures, gear box shaft 2 temperatures and motor bearings A and B temperatures (13 items in all) as the input of the BP neural network. The power of the wind turbine is used as the output for predictions.

It can be seen from Figure 5 that the IBAS-BP algorithm can accurately estimate wind turbine power, which can help us improve our control strategies and maximize the utilization of generators under extreme weather conditions. Through predicting stator and rotor temperatures, the pitches and yaws can be changed in time to avoid possible damage. By means of further reducing power losses of wind turbines, power generation efficiency and our monitoring efficiency can both be further improved.

IV. RESULTS AND DISCUSSION

A. EVALUATION OF MONITORING STANDARDS

The online monitoring of power equipment requires real-time and high efficiency, which places extremely high requirements on the algorithm. For this, we select the number of iterations, average errors (AEs) and average fitness value for evaluation. Among them, the smaller the number of iterations, the shorter the training time of the algorithm and the faster the calculation speed; the smaller the average error value, the higher the prediction accuracy of the model. The average error has been widely used to measure the accuracy of the evaluation algorithm model. When $AE \geq 0.01$, it indicates that the prediction and diagnosis ability of the algorithm is poor.

Timely feedback on the health statuses of equipment requires our algorithm to predict with high enough accuracy, select relative errors and coefficients of determination as the evaluation criteria. Among them, the relative error coefficient can be expressed as follows:

$$E_i = \frac{|y_i' - y_i|}{y_i} \quad (i = 1, 2, \cdots, n) \tag{6}$$

In formula (5), y_i' is the output value predicted by the IBAS-BP model when the i-th sample is used, and y_i represents the real data value of the i-th sample, and n is the number of samples. The smaller the relative error coefficient, the better the sample fitting effect. The coefficient of determination R2 can be expressed as equation (6):

$$R^2 = \frac{(n\sum_{i=1}^{n} y_i' y_i - \sum_{i=1}^{n} y_i' \sum_{i=1}^{n} y_i)^2}{[n\sum_{i=1}^{n} y_i'^2 - (\sum_{i=1}^{n} y_i')^2][n\sum_{i=1}^{n} y_i^2 - (\sum_{i=1}^{n} y_i)^2]} \tag{7}$$

In order to measure the superiority of the IBAS-BP algorithm to establish an intelligent monitoring method, algorithms PSO-BP, BAS-BP and GA-BP are chosen for comparisons (referred to as the IBAS model, the BAS model, the GA model and the PSO model).

The curves of the optimal fitness values of the four algorithms with iteration are shown in Figure 6(a). Figure 6(b) shows the prediction results of the stator and rotor temperatures under the PSO model. Figure 6 (c) shows the prediction

TABLE 3. Algorithm comparison.

Algorithm	Running Time/s (SF_6)	AE	Iterations	MRE (Wind turbine)		R^2(Wind turbine)	
		(SF_6)	(SF_6)	Training%	Test%	Training	Test
GA-BP	339.3	0.71%	73	0.35	0.37	0.9742	0.9475
PSO-BP	275.2	0.72%	44	0.46	0.49	0.9700	0.9502
BAS-BP	34.01	1.08%	18	0.49	0.57	0.9737	0.9383
IBAS-BP	766.8	0.10%	38	0.27	0.25	0.9855	0.9753

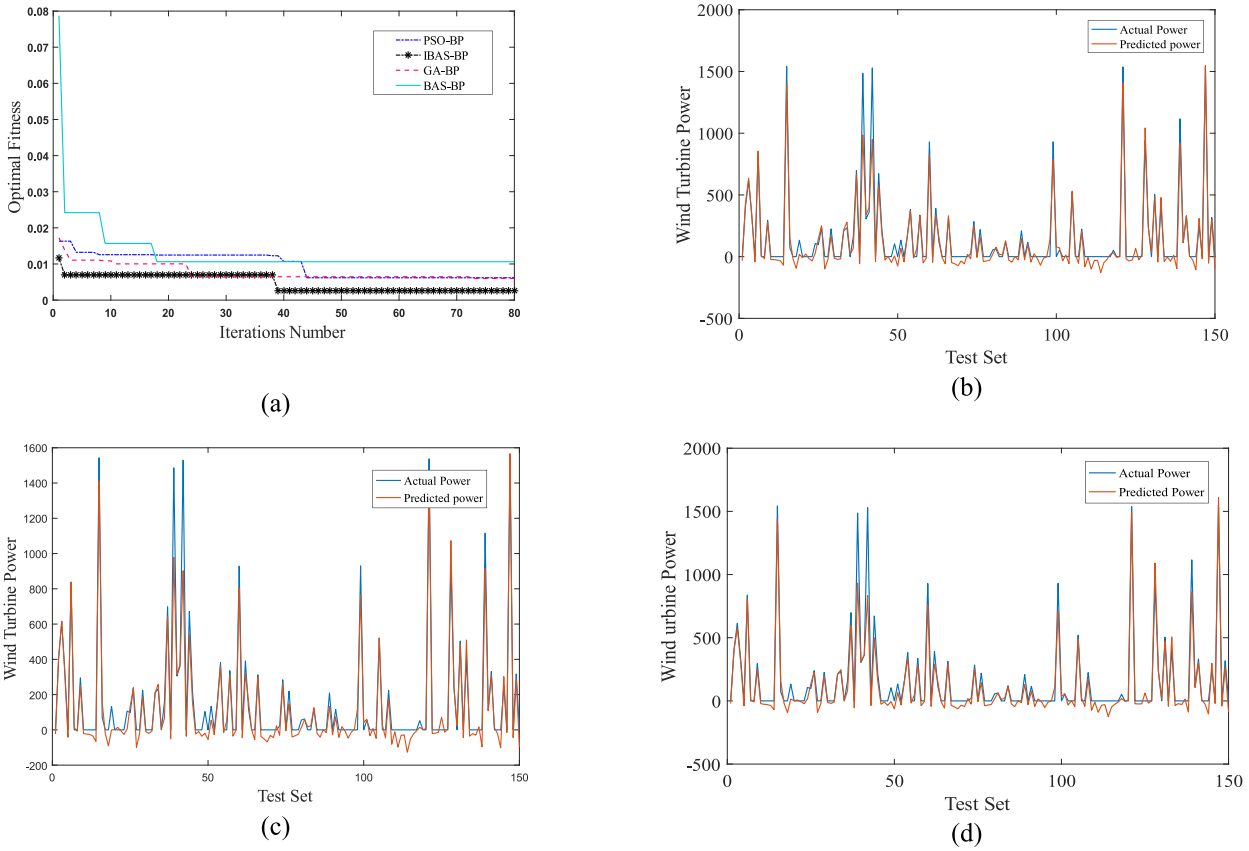

FIGURE 6. (a) Four algorithm fitness curves, (b) Fitting results of testing based on the PSO-BP model, (c) Fitting results of testing based on the GA-BP model (d) Fitting results of testing based on the BAS-BP model.

results of the GA model. Figure 6 (d) shows the prediction results under the BAS model.

Table 3 shows that in the fault diagnosis of the SF6 circuit breaker, the average error (AE) of the IBAS algorithm is only 0.1%, which reflects good robustness. It is better than the average error of the GA-BP algorithm by 0.71% and the average error of the PSO-BP algorithm by 0.72%. However, the BAS-BP algorithm will fall into a local minimum during the iteration process, and the average error is relatively large, which is 1.08%. This proves that the IBAS-BP algorithm has excellent accuracy and response speeds in the field of fault diagnoses. In the power prediction experiment, the IBAS model performs the best in the test set, and the modeling regression determination coefficients R^2 of the training set and testing set are as high as 0.9855 and 0.9753 respectively, which proves better adaptability.

From Figure 5(a), the average number of iterations of the IBAS-BP algorithm is 38, which is lower than 44 times of the PSO model and 78 times of the GA model. Although the iteration speed is faster, the time consumption of the IBAS-BP model is 766.8ms, which exceeds that of the traditional GA-BP (339.3ms) and that of the of the PSO-BP algorithm (275.2ms). The error of the IBAS-BP model is smaller and the accuracy is higher. It can be seen from Figure 5(b) that the predicted values of the PSO model is basically consistent with the actual measured temperatures of the stator and rotor. When the power is higher than 1000W, the model prediction error is too large. In the test set, the relative error coefficient of the PSO model is 0.49%, and R^2 is 0.9502. The performance is lower than the BAS model, which may be related to the insufficient accuracy of the regression surface of the input-output correlation. From Figure 5(c), the GA prediction model has good convergence, but the overall fitting effect is not good. The predicted values are concentrated between 870W and 1240W, which deviates from actual results. In the test set, the relative error coefficient of the model is 0.37%,

and R^2 is 0.9475. In addition, the GA algorithm has complex steps and numerous calculations.

It can be seen from Figure 5(d) that the predicted values of the BAS-BP model are basically consistent with the actual measured values, but, errors will occur in the range of water content greater than 750W and less than 138W. The calculation shows that the relative error coefficient of the BAS-BP model is 0.57%, and determination coefficient R^2 is 0.9383, which has good accuracy and adaptability, but, the experimental effect depends heavily on the locations of the beetles. Compared with Fig 4, the IBAS algorithm is almost completely consistent with the measured data, the error is smaller, and it is very close to the measured data. And in the test set, the relative error coefficient is only 0.25%. Test set determination coefficient R^2 is 0.9753, which reflects good adaptability and further demonstrates the accuracy of the IBAS-BP algorithm and its robustness after parameter optimization. Through comparisons, it can be known that the IBAS model performs best among the four models.

B. MONITORING OPTIMIZATION

Through the training of a large amount of data collected by sensors, the IBAS-BP algorithm can eliminate comprehensive influencing factors under natural conditions. Compared with traditional inspections, the IBAS-BP algorithm not only has smaller training errors but also higher precision and transferability with good nonlinear interpretation modeling ability. With the support of this set of algorithms, power components in the grids can effectively monitor the equipment. But, in changeable environments, how to intelligently avoid risks, build power systems that truly have network collaboration intelligence and cluster evolution capabilities are also problems that need our further exploration. Under extreme weather conditions, how to further improve the accuracy of equipment fault diagnoses and increase the diagnosis speeds of equipment online monitoring is still a big challenge for human beings.

V. CONCLUSION

1) This paper has improved the beetle search algorithm (BAS algorithm) and put forward the notion or concept of the IBAS-BP algorithm for the first time in the academia. Through its application in different scenarios, its universality and robustness of the algorithm is proved.
2) The IBAS-BP algorithm has shown sufficient superiority in the process of being compared with the PSO and GA algorithms. In the SF6 fault diagnosis experiment, the average error is only 0.1%, and the number of iterations is the lowest, 38 times. Compared with traditional algorithms, it takes a longer time of 766.8ms, but it reflects higher accuracy. In the wind turbine power prediction experiment, model regression determination coefficient R^2 can reach 0.9753 and the relative average error is only 0.25%.
3) Sensors are used to realize data collection, signal transmission and make decisions. The IBAS-BP algorithm can realize information exchanges between power systems and consumers. This algorithm can effectively promote the construction of smart grid.

ACKNOWLEDGMENT

The data in this research are provided by Shaanxi Wind Power Plant of China Guodian Corporation, Shaanxi, China.

REFERENCES

[1] M. M. Albu, M. Sanduleac, and C. Stanescu, "Syncretic use of smart meters for power quality monitoring in emerging networks," *IEEE Trans. Smart Grid*, vol. 8, no. 1, pp. 485–492, Jan. 2017.
[2] H. Yi, M. H. Hajiesmaili, Y. Zhang, M. Chen, and X. Lin, "Impact of the uncertainty of distributed renewable generation on deregulated electricity supply chain," *IEEE Trans. Smart Grid*, vol. 9, no. 6, pp. 6183–6193, Nov. 2018.
[3] S. Bhela, V. Kekatos, and S. Veeramachaneni, "Enhancing observability in distribution grids using smart meter data," *IEEE Trans. Smart Grid*, vol. 9, no. 6, pp. 5953–5961, Nov. 2018.
[4] X. Cao, J. Wang, and B. Zeng, "Distributed generation planning guidance through feasibility and profit analysis," *IEEE Trans. Smart Grid*, vol. 9, no. 5, pp. 5473–5475, Sep. 2018.
[5] J.-S. Chou and N.-S. Truong, "Cloud forecasting system for monitoring and alerting of energy use by home appliances," *Appl. Energy*, vol. 249, pp. 166–177, Sep. 2019.
[6] A. Gupta, G. Gurrala, and P. S. Sastry, "An online power system stability monitoring system using convolutional neural networks," *IEEE Trans. Power Syst.*, vol. 34, no. 2, pp. 864–872, Mar. 2019.
[7] P.-Y. Kong, "Cost efficient data aggregation point placement with interdependent communication and power networks in smart grid," *IEEE Trans. Smart Grid*, vol. 10, no. 1, pp. 74–83, Jan. 2019.
[8] C. Arcadius Tokognon, B. Gao, G. Y. Tian, and Y. Yan, "Structural health monitoring framework based on Internet of Things: A survey," *IEEE Internet Things J.*, vol. 4, no. 3, pp. 619–635, Jun. 2017.
[9] J. Qiu, Z. Xu, Y. Zheng, D. Wang, and Z. Y. Dong, "Distributed generation and energy storage system planning for a distribution system operator," *IET Renew. Power Gener.*, vol. 12, no. 12, pp. 1345–1353, Sep. 2018.
[10] H. Wu and M. Shahidehpour, "Applications of wireless sensor networks for area coverage in microgrids," *IEEE Trans. Smart Grid*, vol. 9, no. 3, pp. 1590–1598, May 2018.
[11] H. Ren, B. Hou, G. Zhou, L. Shen, C. Wei, and Q. Li, "Variable pitch active disturbance rejection control of wind turbines based on BP neural network PID," *IEEE Access*, vol. 8, pp. 71782–71797, 2020.
[12] F. Yang, L. Du, W. Chen, J. Li, Y. Wang, and D. Wang, "Hybrid energy harvesting for condition monitoring sensors in power grids," *Energy*, vol. 118, pp. 435–445, Jan. 2017.
[13] J. Zhang, H. Sun, Z. Sun, W. Dong, and Y. Dong, "Fault diagnosis of wind turbine power converter considering wavelet transform, feature analysis, judgment and BP neural network," *IEEE Access*, vol. 7, pp. 179799–179809, 2019.
[14] J. Song, J. Wang, and H. Lu, "A novel combined model based on advanced optimization algorithm for short-term wind speed forecasting," *Appl. Energy*, vol. 215, pp. 643–658, Apr. 2018.
[15] Y. Gao, F. Villecco, M. Li, and W. Song, "Multi-scale permutation entropy based on improved LMD and HMM for rolling bearing diagnosis," *Entropy*, vol. 19, no. 4, p. 176, Apr. 2017.
[16] H. Liu, W. Song, M. Li, A. Kudreyko, and E. Zio, "Fractional Lévy stable motion: Finite difference iterative forecasting model," *Chaos, Solitons Fractals*, vol. 133, Apr. 2020, Art. no. 109632.
[17] H. Liu, W. Song, Y. Niu, and E. Zio, "A generalized cauchy method for remaining useful life prediction of wind turbine gearboxes," *Mech. Syst. Signal Process.*, vol. 153, May 2021, Art. no. 107471.
[18] W. Yao, Y. Zhang, Y. Liu, M. J. Till, and Y. Liu, "Pioneer design of non-contact synchronized measurement devices using electric and magnetic field sensors," *IEEE Trans. Smart Grid*, vol. 9, no. 6, pp. 5622–5630, Nov. 2018.

[19] C. Sun, C. Li, Y. Liu, Z. Liu, X. Wang, and J. Tan, "Prediction method of concentricity and perpendicularity of aero engine multistage rotors based on PSO-BP neural network," *IEEE Access*, vol. 7, pp. 132271–132278, 2019.
[20] Z. Xue, H. Li, Y. Zhou, N. Ren, and W. Wen, "Analytical prediction and optimization of cogging torque in surface-mounted permanent magnet machines with modified particle swarm optimization," *IEEE Trans. Ind. Electron.*, vol. 64, no. 12, pp. 9795–9805, Dec. 2017.
[21] W. Song, C. Cattani, and C.-H. Chi, "Multifractional brownian motion and quantum-behaved particle swarm optimization for short term power load forecasting: An integrated approach," *Energy*, vol. 194, Mar. 2020, Art. no. 116847.
[22] B. Zhang, Y. Duan, Y. Zhang, and Y. Wang, "Particle swarm optimization algorithm based on beetle antennae search algorithm to solve path planning problem," in *Proc. IEEE 4th Inf. Technol., Netw., Electron. Autom. Control Conf. (ITNEC)*, Jun. 2020, pp. 1586–1589.
[23] Y. Zhang, B. Chen, Y. Zhao, and G. Pan, "Wind speed prediction of IPSO-BP neural network based on lorenz disturbance," *IEEE Access*, vol. 6, pp. 53168–53179, 2018.
[24] H. Chaoui, M. Khayamy, O. Okoye, and H. Gualous, "Simplified speed control of permanent magnet synchronous motors using genetic algorithms," *IEEE Trans. Power Electron.*, vol. 34, no. 4, pp. 3563–3574, Apr. 2019.
[25] Y. Kassa, J. H. Zhang, D. H. Zheng, and D. Wei, "A GA-BP hybrid algorithm based ANN model for wind power prediction," in *Proc. IEEE Smart Energy Grid Eng. (SEGE)*, Aug. 2016, pp. 158–163.
[26] J. Li, W. Chen, K. Han, and Q. Wang, "Fault diagnosis of rolling bearing based on GA-VMD and improved WOA-LSSVM," *IEEE Access*, vol. 8, pp. 166753–166767, 2020.
[27] O. Osman, S. Sallem, L. Sommervogel, M. O. Carrion, P. Bonnet, and F. Paladian, "Distributed reflectometry for soft fault identification in wired networks using neural network and genetic algorithm," *IEEE Sensors J.*, vol. 20, no. 9, pp. 4850–4858, May 2020.
[28] S. Wang, J. Wang, F. Shang, Y. Wang, Q. Cheng, and N. Liu, "A GA-BP method of detecting carbamate pesticide mixture based on three-dimensional fluorescence spectroscopy," *Spectrochimica Acta A, Mol. Biomol. Spectrosc.*, vol. 224, Jan. 2020, Art. no. 117396.
[29] Y. Sun, J. Zhang, G. Li, Y. Wang, J. Sun, and C. Jiang, "Optimized neural network using beetle antennae search for predicting the unconfined compressive strength of jet grouting coalcretes," *Int. J. Numer. Anal. Methods Geomech.*, vol. 43, no. 4, pp. 801–813, Mar. 2019.
[30] Q. Wu, H. Lin, Y. Jin, Z. Chen, S. Li, and D. Chen, "A new fallback beetle antennae search algorithm for path planning of mobile robots with collision-free capability," *Soft Comput.*, vol. 24, no. 3, pp. 2369–2380, Feb. 2020.
[31] Y. Cheng, C. Li, S. Li, and Z. Li, "Motion planning of redundant manipulator with variable joint velocity limit based on beetle antennae search algorithm," *IEEE Access*, vol. 8, pp. 138788–138799, 2020.
[32] B. Zhang, C. Wu, Z. Pang, Y. Li, and R. Wang, "Hybrid global optimum beetle antennae search—Genetic algorithm based welding robot path planning," in *Proc. IEEE 9th Annu. Int. Conf. CYBER Technol. Automat., Control, Intell. Syst. (CYBER)*, Jul. 2019, pp. 1520–1524.
[33] Y. Zhang, S. Li, and B. Xu, "Convergence analysis of beetle antennae search algorithm and its applications," 2019, *arXiv:1904.02397*. [Online]. Available: http://arxiv.org/abs/1904.02397
[34] X. Jiang, Z. Lin, T. He, X. Ma, S. Ma, and S. Li, "Optimal path finding with beetle antennae search algorithm by using ant colony optimization initialization and different searching strategies," *IEEE Access*, vol. 8, pp. 15459–15471, 2020.

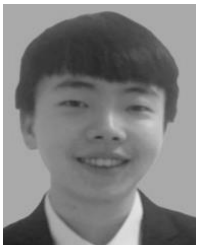

ZHENGGUANG LIU (Student Member, IEEE) was born in Hebei, China, in 2001. He is currently pursuing the bachelor's degree in electrical and electronic engineering with Northwest A&F University, China. He has been working on renewable energy technology and machine learning.

QINYUE TAN (Senior Member, IEEE) was born in Shaoyang, Hunan, China, in 1975. He received the Ph.D. degree in power engineering from the School of Electrical and Electronic Engineering, Huazhong University of Science and Technology (HUST), in 2011. He is currently an Associate Professor with Northwest A&F University. He has always been working on power systems and their automation, power generation via renewable energy, and so on. He also presides over a number of scientific research projects, including the study on the Power Quality and Mechanism of Coupling Between a Nonlinear or Impact Load and Power Grid (the National Natural Science Foundation of China).

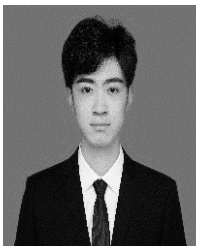

YUBO ZHOU was born in Shandong, China, in 1999. He is currently pursuing the bachelor's degree in electrical and electronic engineering with Northwest A&F University, China. He has been working on power electronics technology.

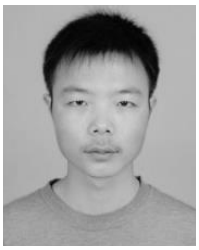

HENGSHAN XU was born in Shaanxi, China, in 1989. He received the Ph.D. degree in power electronics and power drives from North China Electric Power University, Beijing, China, in 2018. His current research interests include active power factor correction (APFC), on-board charger (OBC), and wide gain dc/dc converters in China Three Gorges University.